

Article

Climate Change Characteristics of Typical Grassland in the Mongolian Plateau from 1978 to 2020

Bu He¹, Wulan Tuya^{1,2,3,*}, Si Qinchaoketu^{1,2,3}, Lkhagvadorj Nanzad⁴, Mei Yong^{1,2} , Tang Kesi¹ and Changqing Sun¹

¹ College of Geographical Science, Inner Mongolia Normal University, Hohhot 010022, China

² Key Laboratory of Disaster and Ecological Security on the Mongolian Plateau, Inner Mongolia Autonomous Region, Hohhot 010022, China

³ Key Laboratory of Climate Change and Regional Response on the Mongolian Plateau, Autonomous Region, Hohhot 010022, China

⁴ Information and Research Institute of Meteorology, Hydrology and Environment, Ulaanbaatar 15160, Mongolia

* Correspondence: mtuya1967@163.com

Abstract: Typical grassland is the core of the Mongolian Plateau grassland belt, and is also an important ecological barrier in the north of China. It is of great significance to explore the real-time changes in grassland climate for the prevention and control of climate disasters, and for ecological protection. In this study, the spatial and temporal variation of temperature, precipitation and maximum wind speed in typical Mongolian Plateau grassland were studied using observation data from 16 meteorological stations from 1978 to 2020, using the linear trend method, cumulative anomaly method, Mann-Kendall test, sliding *t*-test and Morlet wavelet analysis. The results show that: (1) The typical grassland temperature has been increasing at a rate of 0.4 °C/10a ($p < 0.001$) over the past 40 years, with the most significant warming in spring and summer; a sudden change from low to high temperature occurred in 1992; the annual average temperature gradually increased from northeast to southwest, with significant warming in the southwest. (2) Annual precipitation decreased slightly at a rate of −2.39 mm/10a, with the most significant decrease in summer precipitation; a sudden change from more to less precipitation occurred in 1998; spatially, precipitation decreased gradually from east to west, with significant moisture reduction in its northern part. (3) The maximum wind speed decreased significantly at a rate of −0.33m/s/10a ($p < 0.001$), with the most pronounced decrease in spring; the maximum wind speed changed abruptly from strong to weak around 1991; spatially, the annual average maximum wind speed decreased gradually from northwest to southeast and northeast, with the most pronounced decrease in the south and northeast. (4) The wavelet analysis shows that the typical grassland area will still be in a warm, low-rainfall and weak-wind stage in the coming years. Using the above analysis, the typical grassland climate of the Mongolian Plateau has shown a clear trend of warm and dry, weak wind in the past 40 years.

Keywords: climate change; spatial and temporal characteristics; mutation detection; wavelet analysis; Mongolian Plateau



Citation: He, B.; Tuya, W.; Qinchaoketu, S.; Nanzad, L.; Yong, M.; Kesi, T.; Sun, C. Climate Change Characteristics of Typical Grassland in the Mongolian Plateau from 1978 to 2020. *Sustainability* **2022**, *14*, 16529. <https://doi.org/10.3390/su142416529>

Academic Editor: Samuel Asumadu-Sarkodie

Received: 9 November 2022

Accepted: 30 November 2022

Published: 9 December 2022

Publisher's Note: MDPI stays neutral with regard to jurisdictional claims in published maps and institutional affiliations.



Copyright: © 2022 by the authors. Licensee MDPI, Basel, Switzerland. This article is an open access article distributed under the terms and conditions of the Creative Commons Attribution (CC BY) license (<https://creativecommons.org/licenses/by/4.0/>).

1. Introduction

Climate change is one of the important environmental issues facing all mankind at present, and is an important topic of concern for international academia and even governments around the world [1]. Since 1990, the Intergovernmental Panel on Climate Change (IPCC) has released six assessment reports with the changes in the global climate system as the focus of attention, and the sixth (2021) assessment report points out that the global average surface temperature increased by 1.09 °C from 2011 to 2020 compared with the pre-industrial level (1850–1990); by the middle of this century, global warming of 1.5 °C is expected, and climate warming will still be increasing [2,3]. Huang et al. [4–6] showed

that global warming is particularly pronounced in arid and semi-arid regions, especially in semi-arid zones, which account for about 44% of global surface warming.

The Mongolian Plateau is located in the interior of Asia and belongs to a typical temperate continental monsoon climate, the main part of which consists of the Inner Mongolia Autonomous Region (Inner Mongolia) of China and Mongolia, and has a significant impact on climate change, both in Asia and globally, due to its unique geographical location, topography and climate characteristics. Most of the Mongolian Plateau is in arid and semi-arid regions with a fragile ecological environment, which is most sensitive to climate change and resulting external disturbances [7,8]. In the past 50 years, the Mongolian Plateau has shown an overall trend of increasing temperature and decreasing humidity, and the warming rate ($0.49\text{ }^{\circ}\text{C}/10\text{a}$) is higher than the global average level ($0.12\text{ }^{\circ}\text{C}/10\text{a}$) [9,10], but there are obvious spatial and temporal differences within the plateau. Since the 1950s, the temperature in Inner Mongolia has continued to rise, precipitation has gradually decreased, and the climate has shown a warm-dry trend [11], with the warm-dry trend being most pronounced in its central and western parts [12,13], where the temperature increase in spring and winter is greater than in other seasons [13]. In recent years, the warm-dry trend has also been significant in Mongolia [9], with the most pronounced occurrence in its eastern part [14], but warm-wet phenomena have occurred in northern and central Mongolia [15,16], and the temperature increase in summer has been most significant [17].

The temperate grassland of the Mongolian Plateau belongs to the eastern part of the temperate steppe belt of Eurasia, with an area of about 2.6 million km^2 , and is an important part of the global ecosystem, playing an important role in the global carbon cycle and the stability of the regional ecosystem [18]. Typical grassland is the core of temperate grassland, mainly distributed in the three provinces of Sukhbaatar, Khentii and Dornod in eastern Mongolia, as well as the eastern part of Xilingol League and the western part of Hulunbeier City in Inner Mongolia of China. In this grassland area, the natural conditions inside and outside the border are the same, including the birthplace of nomadic civilization, with the same arid, disaster-prone and vulnerable characteristics, and the core position of the livestock economy is similar. Therefore, it is still important to study the typical grassland area, regardless of its location, or the ratio of human and animal animals supported by grassland. Under the influence of plateau climate change, the climate of typical grassland area is also susceptible to warm and dry periods [19–21], which directly affect the growth of grassland vegetation. The extreme climate caused by climate change, such as rainstorms and floods [22], high temperature and drought [20], black disaster [23], white disaster [24] and sandstorms [25], even seriously affects the survival and living activities of local people. However, related studies have mainly focused on some areas and some time periods in typical steppe areas [26,27], and cross-border studies covering the entire typical steppe areas in China and Mongolia have not been covered. At the same time, previous studies mostly focus on the longitudinal variation of a single climate element, and mostly use a single detection method, which lacks the verification of detection results. In addition, most of the related studies were around 2010 and do not cover the climate change in the last decade. However, previous studies by Qin [28] and Dan [29] also found that climate change on the Mongolian Plateau fluctuated dramatically after 1975. Therefore, this study analyzes the spatial and temporal characteristics of temperature, precipitation and maximum wind speed in the study area for the past 40 years, based on the observations of 16 meteorological stations in the typical grassland area of the Mongolian Plateau from 1978 to 2020, using the linear trend method, cumulative anomaly method, Mann-Kendall test, sliding t -test, and Morlet wavelet analysis to find the mesoscale abrupt change phenomenon and cyclical pattern of the plateau climate change, with a view to providing reference for the ecological restoration of grassland vegetation in the Mongolian Plateau and the sustainable development of regional livestock industry.

2. Study Area

The study area mainly includes the eastern part of Xilingol League and the western part of Hulunbeier City in Inner Mongolia of China, and Sukhbaatar and Dornod provinces in Mongolia, with a total area of about 4×10^5 km² (Figure 1). The landscape type in the region is high plains and low hills, and the overall topography gradually decreases from southwest to northeast, with an elevation between 485 and 1870 m. It belongs to the temperate continental monsoon climate zone, with warm summers and cold winters. The annual average temperature increases gradually from northeast to southwest, with an annual average temperature of 1.2 °C and a large annual temperature difference. The terrestrial vegetation is typical grassland, and the terrestrial soil is chestnut-calcium soil, and there is also a small amount of wind-sand soil. The main rivers and lakes are Kherlen River, Halkh River, Silin River, and Hurun Lake, and Buir Lake, etc. The typical grasslands have served as the feed base for grazing livestock and wild animals, which is mainly fixed grazing in the territory and nomadic outside the territory.

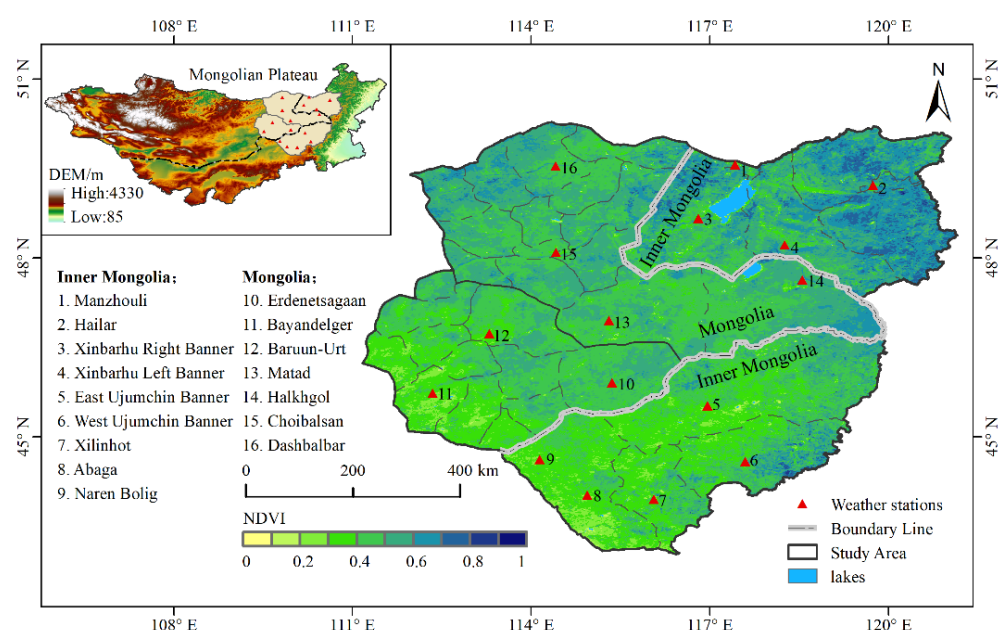


Figure 1. Map of typical grassland area and distribution of meteorological stations. The background is the average NDVI in August 2020.

3. Data and Methodology

3.1. Data

In this study, the selected data are the monthly average temperature, precipitation and maximum wind speed observations of 16 meteorological stations (9 meteorological stations in Inner Mongolia and 7 meteorological stations in Mongolia, shown in Figure 1) in the typical grassland of Mongolian Plateau from 1978 to 2020. The meteorological data within the country were obtained from the Chinese meteorological data network (<http://data.cma.gov.cn> accessed on 3 August 2021), and those outside the country were obtained from the Mongolian meteorological data network (<http://tsag-agaar.mn/> accessed on 15 September 2021). The spatial values of climate elements were obtained by Kriging spatial interpolation under ArcGIS environment, based on the information of latitude and longitude of meteorological stations, and the characteristics of climate change in typical grassland on the Mongolian Plateau in the past 40 years were analyzed. Among them, temperature and maximum wind speed data of each season were obtained by a weighted average of the values of corresponding months, and precipitation data were obtained by weighting the values of corresponding seasons and months. The four seasons are divided into spring (March to May), summer (June to August), autumn (September to November), and winter (December to February of the following year).

3.2. Methodology

3.2.1. Univariate Linear Regression Analysis

In order to understand the long-term trend of climate elements in typical grassland, a univariate linear regression model was used to describe the long-term trend of temperature, precipitation and maximum wind speed. Univariate linear regression analysis is the simplest linear regression model; its purpose is to establish the linear relationship between x and y , and describe its linear trend. The calculation formula is [30]:

$$y = b + at \quad (1)$$

where y is the climate element series, t is the time series (1978–2020), b is the regression constant, a is the regression coefficient (slope), and $10a$ is the climate tendency rate of climate elements every 10 years; if $a > 0$, it indicates an upward trend of climate elements; if $a < 0$, it indicates a downward trend.

3.2.2. Mutation Detection

Abrupt climate change is an important phenomenon prevalent in the climate system, a jump in climate from one steady state to another, manifested as a sharp change in climate from one statistical characteristic to another in space and time [31]. There are many methods to test for abrupt change. In this study, the cumulative anomaly test, Mann-Kendall test and sliding t -test are mainly adopted to analyze the abrupt change of the time series of climate elements in the study area, so as to achieve the effect of mutual comparison and mutual verification. When one of the methods is inconsistent with the other two, the year of mutation is determined by the principle of majority rule. Among them, both the Mann-Kendall test and sliding t -test methods set the confidence line at 0.05 significance level.

The cumulative anomaly is a method to intuitively judge the trend of climate change from the curve. For the climate element sequence x , the cumulative anomaly at a certain time t is expressed as [30]:

$$x = \sum_{i=1}^t (x_i - \bar{x}) \quad t = 1, 2, \dots, n \quad (2)$$

$$\bar{x} = \frac{1}{n} \sum_{i=1}^n x_i \quad (3)$$

where the cumulative anomaly values at n moments will be calculated to draw the cumulative anomaly curve and analyze the change trend of climate factors.

The Mann-Kendall mutation test, proposed by Mann and Kendall, is a nonparametric statistical test recommended by the World Meteorological Organization (WMO), which is widely used worldwide. Its advantages are that it does not require samples to follow a certain distribution and is not disturbed by a few outliers, and it can accurately identify mutation characteristics and mutation points on time series [32]. In addition, the calculation method is simple and has been used by many scholars to analyze the mutation analysis of time series of meteorological, runoff, and sediment elements [33–35]. Therefore, the study conducted a Mann-Kendall mutation test on the annual average temperature, annual precipitation and annual average maximum wind speed of typical grassland by programming in MATLABR2018b software. The calculation procedure is detailed in the reference [30].

The sliding t -test is used to test whether the difference between the means of two sample groups is significant to test for mutation, for which the continuous series is divided into two end subsequences, and if the difference between the means of the two subsequences exceeds a certain significance, it can be assumed that the mean has undergone a qualitative change and a mutation has occurred. In this study, the reliability of the calculation results was improved by iteratively adjusting the subsequence length in order to avoid any selection of subsequence length causing the drift of mutation points, and the selected

subsequence length in the paper was 10 years. The calculation procedure is detailed in the reference [36].

3.2.3. Morlet Wavelet Analysis

Morlet wavelet analysis is a tool to study the long-term change of climate elements, which is widely used in the field of meteorology. It can reveal the transformation characteristics and periodicity of climate elements in a time series, and wavelet square difference can reveal the main period of climate elements in a time series [37]. Therefore, Morlet wavelet analysis was used to understand the periodicity of annual average temperature, annual precipitation and annual average maximum wind speed in typical grassland. The calculation procedure is detailed in reference [30].

4. Results

4.1. Temporal Variation Characteristics of Temperature, Precipitation and Maximum Wind Speed

4.1.1. Interannual and Seasonal Variations in Temperature, Precipitation and Maximum Wind Speed

Figure 2 shows the annual average temperature, precipitation and maximum wind speed of all meteorological stations in the typical grassland. As seen in Figure 2a, the annual average temperature of typical grassland showed a significant upward trend in the past 40 years, and the climate tendency rate was $0.4\text{ }^{\circ}\text{C}/10\text{a}$ ($p > 0.001$), which is significantly higher than the global annual average temperature warming rate ($0.12\text{ }^{\circ}\text{C}/10\text{a}$) [38]. The annual average temperature anomaly curves showed that the temperature was mainly negative during the periods 1978–1993 and 2009–2013, and positive during the periods 1994–2008 and 2014–2020, among which the anomaly values in 2007, 2014 and 2019 all exceeded $+1\text{ }^{\circ}\text{C}$, and even the anomaly value in 2007 was nearly $+2\text{ }^{\circ}\text{C}$. It can be seen that climate warming has accelerated in the past 10 years. From the trend of temperature change in each season (Figure 3a, Table 1), the average temperature in all seasons showed an increasing trend, with the largest warming in spring at $0.62\text{ }^{\circ}\text{C}/10\text{a}$ ($p < 0.001$); the smallest in winter at $0.15\text{ }^{\circ}\text{C}/10\text{a}$; $0.49\text{ }^{\circ}\text{C}/10\text{a}$ ($p < 0.001$) and $0.35\text{ }^{\circ}\text{C}/10\text{a}$ ($p < 0.01$) in summer and autumn, respectively. Among them, the warming in spring and summer was, however, higher than the average of $0.37\text{ }^{\circ}\text{C}/10\text{a}$ in spring and $0.27\text{ }^{\circ}\text{C}/10\text{a}$ in summer for the whole Mongolian Plateau (1961–2014) [28], indicating that the warming of the typical grassland climate was mainly caused by the warming in spring and summer. In particular, a significant increase in temperature after the mid-late 1990s has led to an increase in the warming of typical grassland vegetation during the growing season.

Table 1. Trends of annual and seasonal temperature, precipitation, and maximum wind speed in typical grasslands.

Climate elements	Spring	Summer	Autumn	Winter	Interannual
temperature ($^{\circ}\text{C}/10\text{a}$)	0.62 ***	0.49 ***	0.35 **	0.15	0.4 ***
precipitation (mm/10a)	2.33	−7.08	1.46	0.91 **	−2.39
maximum wind speed (m/s/10a)	−0.72 ***	−0.19	−0.22	−0.16	−0.33 ***

Note: **, ***, indicate significance tests at 0.01, 0.001, respectively.

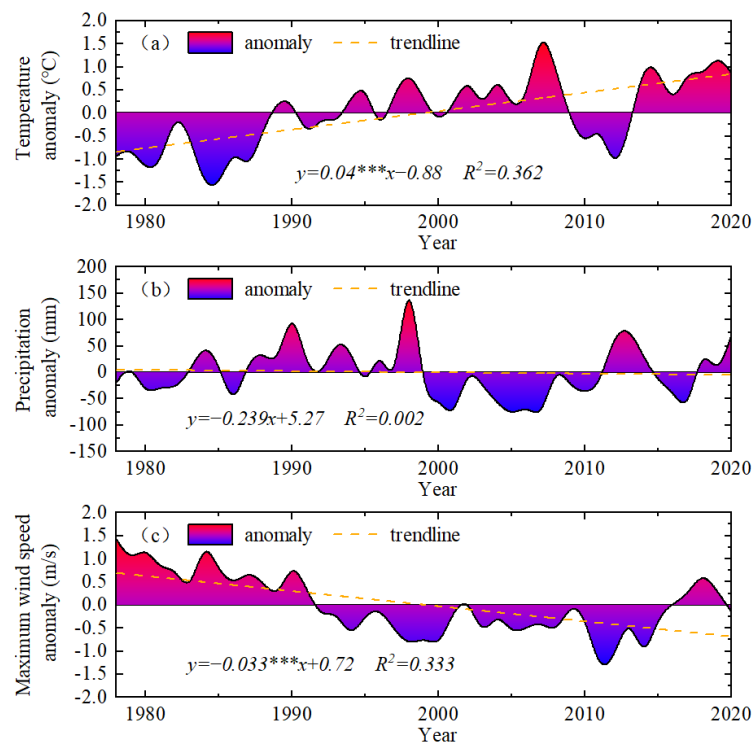


Figure 2. Interannual variation of temperature (a), precipitation (b) and maximum wind speed (c) in the typical grassland, (***) at 0.001 level of significance).

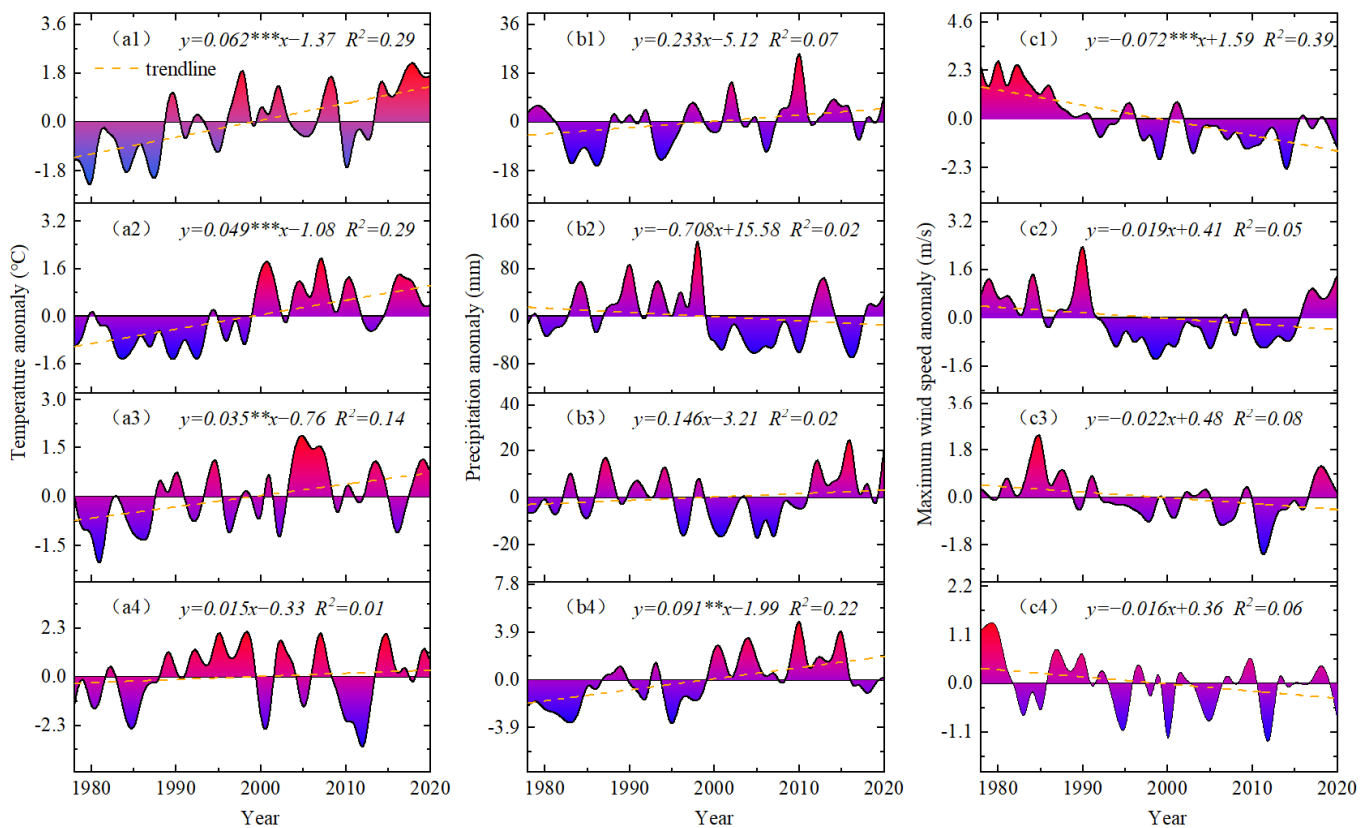


Figure 3. Seasonal variation of temperature (a), precipitation (b) and maximum wind speed (c) in the typical grassland; 1—spring, 2—summer, 3—autumn, 4—winter; (**, ***) at 0.01, 0.001 level of significance, respectively).

As seen in Figure 2b, the typical steppe annual precipitation has shown a weak decreasing trend in the last 40 years, with a climatic tendency rate of -2.39 mm/10a, which is the same as the decreasing trend of annual precipitation across the Mongolian Plateau [10]. The average precipitation in each season showed different trends and intensity of changes: the precipitation in spring, autumn and winter all showed an increasing trend, among them the largest rise in the spring precipitation for the 2.33 mm/10a, autumn and winter, respectively, is 1.46 mm/10a and 0.91 mm/10a ($p < 0.01$). Summer precipitation showed a decreasing trend of -7.08 mm/10a (Figure 3b, Table 1), which was consistent with the decreasing trend of annual precipitation. The obvious decrease in summer precipitation is the main factor leading to the trend of aridification of the climatic environment in typical steppe areas. In addition, natural disasters such as floods and droughts, which are easily formed, pose serious hazards to the growth of grassland vegetation and the development of the local livestock industry.

The annual average maximum wind speed of the typical grassland showed a significant downward trend in the past 40 years, with a climate tendency rate of -0.33 m/s/10a ($p < 0.001$) (Figure 2c). From the distance level curve of the annual average maximum wind speed, it can be seen that the maximum wind speed in the typical grassland area has shown a significant decline since the early 1990s, and the distance level of the maximum wind speed was negative from 1992 to 2015, including 12 years with a distance level above -0.5 m/s, and the distance level even exceeded -1 m/s in 2011, 2012 and 2014. As seen in Figure 3c and Table 1, the average maximum wind speed in all seasons showed a decreasing trend, with the largest decrease of 0.72 m/s/10a ($p < 0.001$) in spring, followed by 0.22 m/s/10a in autumn, 0.19 m/s/10a in summer, and the smallest decrease of 0.16 m/s/10a in winter. From about the early 1990s, the average maximum wind speed of all seasons showed a decreasing trend, and the time scale was basically consistent with the decreasing trend of the annual average maximum wind speed. The obvious decrease in mean maximum wind speed in spring reduces the occurrence of typical grassland dust events and reduces surface evaporation, thus contributing to the natural restoration of grassland vegetation.

4.1.2. Abrupt Change Detection of Annual Average Temperature, Annual Precipitation and Annual Average Maximum Wind Speed

The study used three abrupt change monitoring methods, including the Mann-Kendall test (M-K test for short), cumulative distance level and sliding t -test, to finally determine the abrupt change years of typical grassland annual average temperature, annual precipitation and annual average maximum wind speed. In the M-K test, the UF curve is the time series statistical curve (UF curve for short) and the UB curve is the inverse time series statistical curve (UB curve for short); $UF > 0$ means that the series has an upward trend; $UF \leq 0$ means a downward trend, the intersection of the two curves is the climate change mutation point, and if UF exceeds the critical line of 0.05 it represents a more significant time series change trend. The results are shown in Figure 4 and 5, and Table 2.

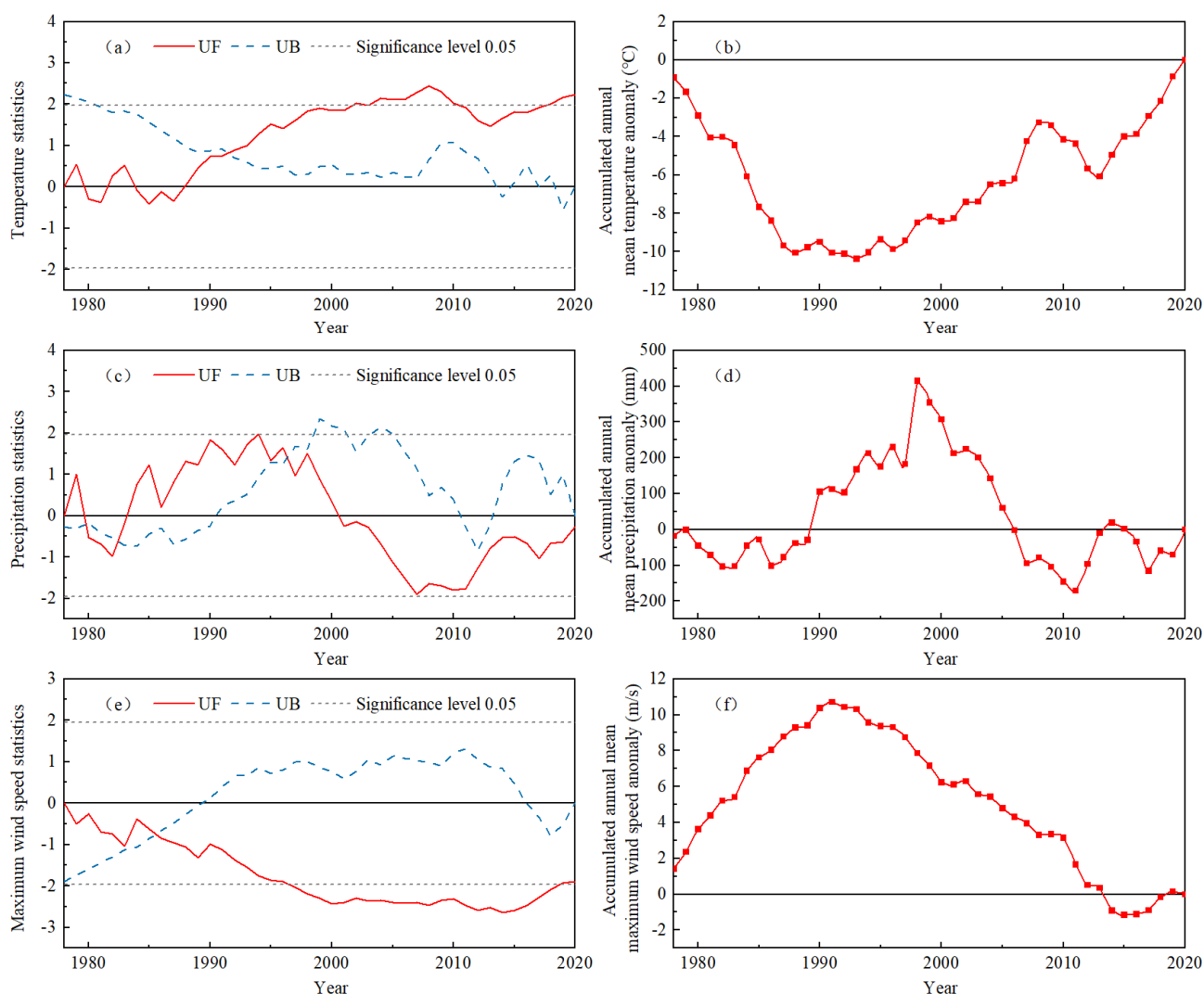


Figure 4. Mann-Kendall mutation test (a,c,e) and cumulative anomalies (b,d,f) of annual average temperature, annual precipitation, and annual average maximum wind speed in typical grassland.

Table 2. Mutation years of annual average temperature, precipitation and maximum wind speed in typical grasslands.

Climate Elements	Mann-Kendall Test	Cumulative Anomaly Test	Sliding <i>t</i> -Test	Mutation Year
temperature	1991–1992 year	1993 year	1992 year	1992 year
precipitation	1980, 1983, 1997 year	1998, 2011 year	1998 year	1998 year
Maximum wind speed	1985–1986 year	1991 year	1991 year	1991 year

As seen in Figure 4a, the UF curve fluctuated and changed repeatedly around the value of 0 from 1978 to 1989, and after 1989 the overall value lies above the value of 0, indicating an upward trend in the temperature time series, which passed the significance level of 0.05 in 2002 and started a significant upward trend. The UF and UB curves have an intersection in the confidence zone, indicating that the sudden temperature change occurred in 1991–1992. In order to test the reliability of the results, the cumulative anomaly test and the sliding *t*-test were selected in this study. According to the results of the cumulative anomaly test (Figure 4b), the annual average temperature anomaly value was almost continuously negative before 1993, and continued to be positive after 1993, indicating that the years before and after 1993 were two periods of relatively low and high temperature, respectively. The results of the sliding *t*-test (Figure 5a) show that the annual average temperature had

a sudden warming process in 1992. According to the three test results (Table 2), it can be judged that the annual average temperature underwent a sudden change from low to high temperature in 1992.

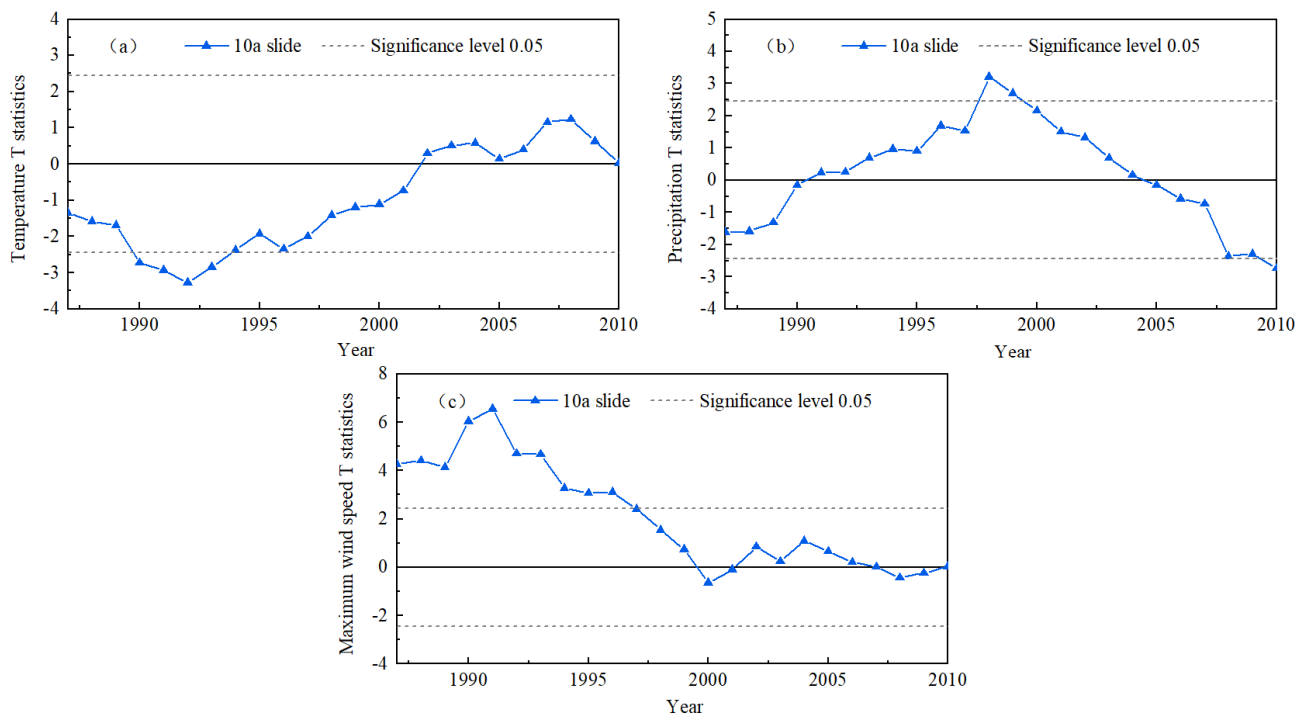


Figure 5. Sliding t -test of typical grassland meteorology; (a)—annual average temperature, (b)—annual precipitation, (c)—annual average maximum wind speed.

The results of the M-K test for annual precipitation (Figure 4c) show that the UF curve shows a fluctuating decrease from 1978 to 2020, After 2000, the overall UF curve was below 0, but failed to pass the significance level of 0.05. UF and UB curves have three intersection points in the confidence region, which are 1980, 1983 and 1997, respectively. The results of the cumulative anomaly test show that (Figure 4d) the cumulative anomaly value of annual precipitation shows an obvious rise and fall process, reaching the peak and valley values in 1998 and 2011, respectively. The peak value indicates that there are two periods of more and less precipitation before and after 1998, and the valley value the is opposite. According to the results of the sliding t -test (Figure 5b), there was a sudden process of precipitation reduction near 1998. With the results of the three tests (Table 2), it can be determined that a sudden change in annual precipitation from more to less occurred in 1998.

The results of the M-K test for the annual average maximum wind speed (Figure 4e) show that the UF curve is generally below the value of 0, indicating that the maximum wind speed shows a downward trend in the time period, and passes the significance level of 0.05 in 1997, which starts a significant downward trend. UF and UB curves intersect in the confidence region in 1985–1986. According to the verification results of cumulative anomalies (Figure 4f), the cumulative anomaly value of annual average maximum wind speed showed a trend of first rising and then declining, and the turning point was in 1991, indicating that there were two periods of strong and weak maximum wind speed around 1991. Firstly, by comparing the results of the above two tests, it is found that there are time differences in the mutation points. Therefore, the study uses the sliding t -test to verify the results and finds that the annual maximum wind speed changed from strong to weak around 1991 (Figure 5c, Table 2).

4.1.3. Periodic Variation of Annual Average Temperature, Annual Precipitation and Annual Average Maximum Wind Speed

In the wavelet coefficient real part contour plot, the horizontal axis is time (year), the vertical axis is a time scale, and the contour is the wavelet coefficient real part value. When the wavelet coefficient real part is positive (red area), it indicates a warm period, a wet period, and a strong wind period, and when the wavelet coefficient real part is negative (blue area), it indicates a cold period, dry period, and a weak wind period. On the other hand, the wavelet variance indicates the distribution of the energy of periodic fluctuations in the time series of temperature, precipitation, and maximum wind speed on the time scale. The results are shown in Figure 6.

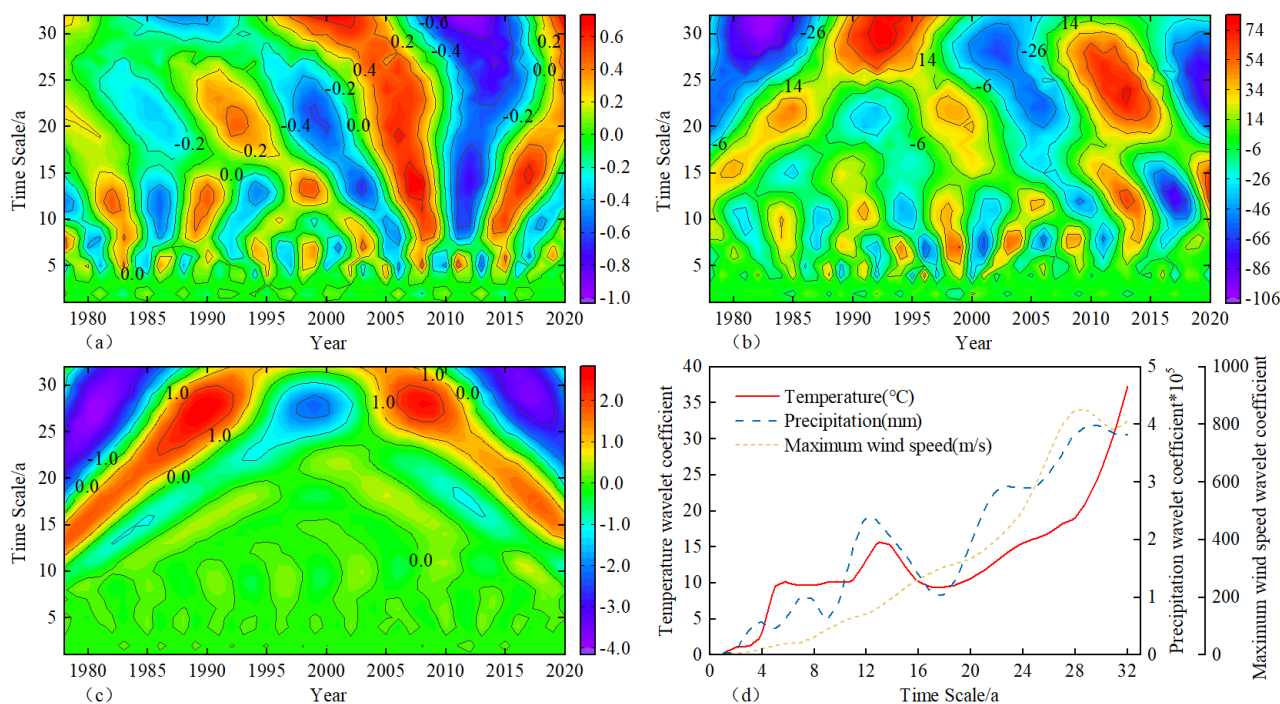


Figure 6. Wavelet coefficient real part contour plots (a,b,c) and wavelet variance plots (d) of annual average temperature, annual precipitation, and annual average maximum wind speed in typical grasslands.

As seen in Figure 6a, the annual average temperature shows multi-timescale characteristics in the process of change, and there are three types of scales of cyclical changes, among which quasi-2 oscillations with alternating high and low on the 30–32 years scale, quasi-6 oscillations on the 12–14 years scale and 5–6 years scale quasi-10 oscillations occur, and all three scales have a full range of periodic variations. The wavelet variance curves show that there are extreme values of the wavelet variance of the annual average temperature at 6, 13 and 32 years, with the strongest time-scale cycle oscillation at 32 years, which is the first main cycle of temperature variation (Figure 6d). According to the results of the 32-year oscillation cycle analysis, it can be seen that the current temperature in the typical grassland area is warm, and the 32-year oscillation cycle has not finished yet, so it can be presumed that the typical grassland area is still in the warm phase in the future period.

The wavelet coefficient results (Figure 6b) exhibited four types of scales of periodic variation in annual precipitation during the variation process, among which are quasi-3 oscillations with alternating high and low on the 26–32 year scale, quasi-4 oscillations on the 19–24 year scale, quasi-6 oscillations on the 9–13 year scale and quasi-9 oscillations on the 6–7 year scale, with the first three scales having a region-wide cyclical variation. As can be seen from Figure 6d, the annual precipitation wavelet variance curves have extreme values at 7, 12, 23 and 29 years, with the maximum peak at the 29-year time scale, which is

the first main cycle of precipitation variation. Based on the analysis results of the 29-year oscillation cycle, it is inferred that the typical grassland area is currently in a drought phase and will continue for some time.

The wavelet coefficient results (Figure 6c) showed a 23–32-year stable cyclic variation in the annual mean maximum wind speed during the variation, with a quasi-3 oscillation of alternating highs and lows, with a full range. As can be seen from Figure 6d, there is only one obvious peak in the wavelet variance curve of the annual average maximum wind speed in the past 40 years, corresponding to the strongest oscillation of the 28-year time scale cycle, which is the first main cycle of the maximum wind speed variation. From this, it can be inferred that the typical grassland area is in a weak wind phase, and that the phase will still last for some time.

4.2. Temporal Variation Characteristics of Temperature, Precipitation and Maximum Wind Speed

4.2.1. Spatial Variation of Temperature

Figure 7a shows the spatial distribution of the annual average temperature of the typical grassland. The annual average temperature in the past 40 years gradually increased from northeast to southwest, with obvious longitudinal and latitudinal zonation characteristics and temperature variations of -0.53 – 3.1 °C. The lower temperature area is located in the central part of Hulunbeier City, with an annual average temperature of less than 0 °C. The higher area is found in the central part of Xilingol League, with an annual average temperature greater than 2.5 °C. From the spatial trend of temperature change, the temperature in all regions showed an increasing trend, and the warming rate increased from northeast to southwest: the warming rate in the north and northeast of the steppe area was smaller, with Matad in the Dornod Province as the area with the smallest warming rate (0.26 °C/10a). The warming rate in the south and west was larger, and the warming center appeared in Abaga Banner of Xilingol League (0.6 °C/10a).

As seen in Figure 7a1–a4, the spatial distribution of seasonal temperature in typical grassland is similar to that of annual average temperature, and the spatial difference of seasonal temperature is obvious, which is shown as increasing gradually from northeast to southwest. However, it is worth noting that the Kriging interpolation effect of summer temperature in Figure 7a2 is not ideal, which indicates that the temperature difference between meteorological stations in summer is small, so the spatial difference of summer temperature is not significant. The spatial variation trend of temperature in each season shows that the spatial variation of temperature warming rate in the four seasons is consistent with the annual average temperature change, which is also increasing from northeast to southwest: the region with a higher warming rate is the southwest; the smaller area is the northeast. The maximum warming rate is observed in spring (Figure 3a), and the maximum warming rate occurred in Abaga Banner of Xilingol League (0.79 °C/10a). The minimum value was Hailar District of Hulunbeier City (0.46 °C/10a) (Figure 7a1).

Overall, the spatial distribution of interannual and seasonal high temperature centers and warming centers in typical grassland is roughly similar, i.e., they occur in the southwestern part of the typical grassland area, indicating that the closer to the drought center, the stronger the warming is, and the opposite is weaker.

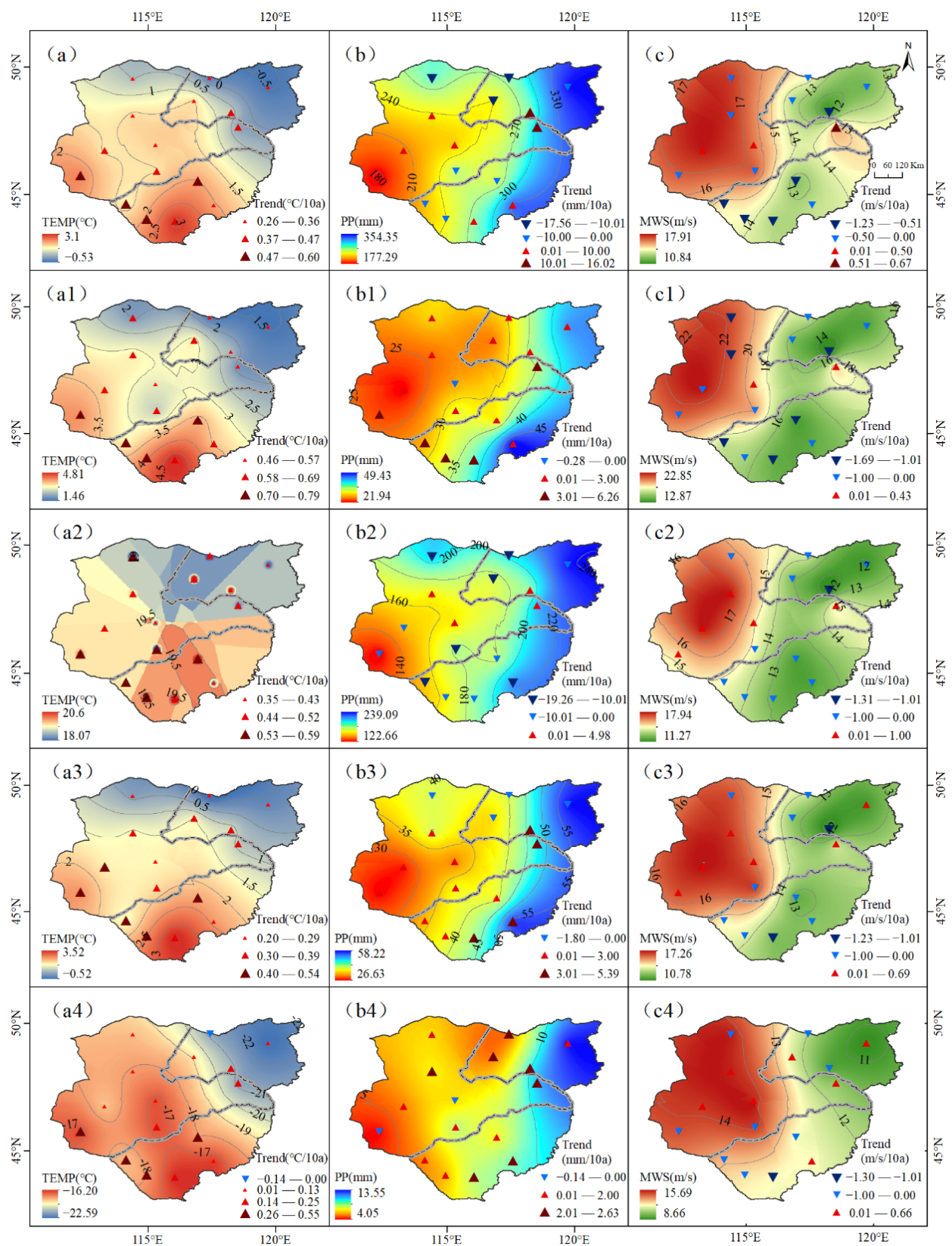


Figure 7. Spatial distribution and spatial variation characteristics of temperature, precipitation and maximum wind speed in typical grassland ((a)—average annual temperature, (b)—annual precipitation, (c)—average annual maximum wind speed: (1)—spring, (2)—summer, (3)—autumn, (4)—winter).

4.2.2. Spatial Variation of Precipitation

The spatial distribution of annual precipitation is plotted in Figure 7b, which gradually decreases from the east to the west, with obvious longitude zonal characteristics, and precipitation variations of 177.29–354.35 mm. Areas with more precipitation are located in Hulunbeier City, the eastern section of Xilingol League and the southeastern part of Dornod Province, where annual precipitation reaches more than 300mm. Lesser areas are found in the western part of Sukhbaatar Province, where annual precipitation is less than 210 mm. From the spatial trend of precipitation change, the tendency rate of precipitation shows a decreasing-increasing-decreasing trend from north to south: precipitation decreases in the south and north of the grassland area, and the center of decreasing wetness appears in Manzhouli of Hulunbeier City (-17.56 mm/10a); precipitation increases in the middle and local areas in the south, and the center of increasing wetness is in the Halkhgol area of Dornod province (16.02 mm/10a).

As seen in Figure 7b1–b4, the spatial distribution of precipitation in each season of a typical grassland is similar to that of annual precipitation, which shows a gradual decrease from east to west. Compared with the other three seasons, the trend of summer precipitation is similar to the trend of annual precipitation decrease (Figure 3b), and the spatial variation pattern of both is also basically the same: the regions with a large decrease in summer precipitation are the northern and southern parts of the grassland area, with the maximum decrease occurring in Manzhouli of Hulunbeier City (-19.26 mm/10a); the regions with an increasing trend in summer precipitation are the central part, with the maximum increase occurring in the Matad area of Dornod Province (4.98 mm/10a) (Figure 7b2).

Overall, the decrease in annual precipitation in typical grassland is mainly caused by the decrease in summer precipitation, and the decrease in precipitation is obvious in the south and north of the grassland area, and the decrease is greater in the north than in the south.

4.2.3. Spatial Variation of Maximum Wind Speed

The spatial distribution of the annual average maximum wind speed is plotted in Figure 7c, which gradually decreases from northwest to southeast and northeast, with obvious longitude zonation characteristics, and the maximum wind speed varies from 10.84–17.91 m/s. The stronger areas of maximum wind speed are located in Sukhbaatar Province and the western part of Dornod Province, both reaching more than 17 m/s. Weaker areas are found in the western part of Hulunbeier City and the central part of Xilingol League, where the maximum wind speed is less than 14 m/s. From the spatial trend of maximum wind speed change, the maximum wind speed showed a decreasing trend except for the local areas in the middle of the typical grassland (Halkhgol, Matad, Baruun-Urt, etc.), which showed an increase. Among them, the decrease in the maximum wind speed was greater in the weaker areas than in the stronger ones: the maximum decrease occurred in Xilinhot of Xilingol league and Xinbarhu Left Banner of Hulunbeier City (-1.23 m/s/10a), while the maximum increase occurred in the Halkhgol area of the Dornod Province (0.67 m/s/10a).

As seen in Figure 7c1–c4, the spatial distribution of the average maximum wind speed in each season is similar to that of the annual average maximum wind speed, which shows a gradual decrease from northwest to southeast and northeast, but there are spatial differences in the change trends. Of all seasons, the maximum wind speed decreased the most in spring (Figure 3c), and regionally it decreased except for in areas such as Matad and Halkhgol in the Dornod Province of Mongolia. The maximum decrease occurred in Xinbarhu Left Banner in Hulunbeier City (-1.69 m/s/10 years) (Figure 7c1).

Overall, the decrease in the annual average maximum wind speed of typical grassland was mainly caused by the decrease in the maximum wind speed in spring, and the decrease was most obvious in the southern and northern parts of the grassland area. In particular,

the decrease in the Inner Mongolia grassland area was greater than that in the Mongolian grassland area.

5. Discussion

The results of the study showed that the annual average temperature of a typical grassland on the Mongolian Plateau in the last 40 years showed a significant increasing trend, precipitation showed a slight decreasing trend, and maximum wind speed showed a significant decreasing trend: the annual average temperature increased at a rate of $0.4\text{ }^{\circ}\text{C}/10\text{a}$ ($p < 0.001$), the annual precipitation decreased at a rate of $-2.39\text{ mm}/10\text{a}$, and the annual average maximum wind speed decreased at a rate of $-0.33\text{ m/s}/10\text{a}$ ($p < 0.001$) rate, which is consistent with the trend of climate change in the Mongolian Plateau [28,39].

Climate change in the typical grassland of the Mongolian Plateau is related but not identical to the climate of the Mongolian Plateau as a whole, and although both are in the warming phase, the warming rate in the grassland area is slightly higher than that of the whole plateau [28], indicating that the typical grasslands are very sensitive to the global warming response. The study found that the typical grassland warming rate gradually increased from northeast to southwest, with the most pronounced warming in the southwest, which is consistent with the results of the climate change studies of Tong [12] and Ma [40] et al. in Inner Mongolia, indicating that the closer to the drought center, the stronger the warming rate. The seasonal variation, with a greater rate of temperature rise in spring and summer, is consistent with earlier findings [41], but is slightly different from the Mongolian Plateau, where the most pronounced temperature rise occurs in winter [28], thus reflecting the spatial variability of the plateau. For precipitation, the trend of decreasing annual precipitation in typical grassland over the past 40 years is consistent with the findings of Qin [10] and Dan [29] et al. However, the magnitude of the decrease is slightly different, which may be related to the inconsistency of the selected study area and time period. Dan [29] concluded that the annual precipitation of the Mongolian Plateau declined at a rate of $-6\text{ mm}/\text{decade}$ during 1976–2010, using the linear trend method. The study was easily affected by extreme values, so the decrease in precipitation was slightly exaggerated. The study found that the decrease in annual precipitation in typical grasslands was caused by a decrease in summer precipitation, with the greatest decrease in the north and south, which is consistent with previous studies [10]. Among them, the decrease in precipitation in the north may be related to the temperature increase in the northern hemisphere in the circum-Baikal region, and related studies have shown that the continuous increase in surface temperature in this region after 1996 has led to a decrease in the longitudinal gradient of convective temperature and vertical shear of latitudinal winds in the Mongolian Plateau, thus weakening the oblique atmospheric pressure in the troposphere and making it easy to maintain a warm anomalous anticyclonic circulation, a decrease in the frequency of cyclone activity in the circum-Baikal region and a decrease in summer precipitation in the Mongolian Plateau [42,43]. Since the 1970s, the weakening of East Asian monsoon circulation has reduced the transport of water vapor into the mainland, resulting in the decrease in precipitation in the eastern and southeastern parts of the Mongolian Plateau [44,45]. For the maximum wind speed, a significant decrease dominated in spring, which had the greatest impact on the evolution of the annual trend, especially in the typical grasslands of Inner Mongolia (Hulunbeier City and Xilingol League), and this result is consistent with the results of the study by Zhang [39] on the changes of the spatial and temporal characteristics of the maximum wind speed in Inner Mongolia. The decrease in the maximum wind speed may be related to the weakening of the East Asian winter and summer winds due to the eastward shift and weakening of the East Asian trough in the context of global warming due to the decrease in the difference in sea-level pressure and near-surface temperature between the Asian continent and the Pacific Ocean [46].

In addition, the abrupt changes of temperature, precipitation and maximum wind speed (Figure 4) show that the abrupt changes of the three points are consistent in time,

that is, the abrupt changes occurred roughly in the late 1990s, which is similar to the results of previous studies on the abrupt changes of Mongolian Plateau climate [40,47]. However, it significantly lags behind Northeast China, especially with the sudden change in precipitation with a significant lag of nearly 15 years [30]. There is a large-scale change of about 30 years in the cycle of temperature, precipitation and maximum wind speed in the typical grassland, and the climate type changes from cold and wet, strong wind type to warm and dry, weak wind type climate, and the typical grassland climate is currently in the warm and dry, weak wind period, and the trend will continue for some time, which further confirms the findings of Tong et al. [47] on the continuous warm and dry climate of the typical grassland in Inner Mongolia. The warm and dry climate will trigger accelerated evaporation from water surfaces, reduced precipitation, and increased natural disasters such as droughts and dust storms, leading to severe degradation of grassland vegetation, which in turn will affect the stable development of livestock production in grassland areas [48–50]. In particular, the intensification of warm drying in summer causes a rapid decrease in summer precipitation, which aggravates drought stress in grassland plants [51], leading to the closure of plant stomata and inhibiting normal plant growth [52], thus bringing serious harm to grassland ecology. In addition, the decrease in maximum wind speed can reduce the erosion and transport capacity of wind, which is beneficial to the fixation of grassland vegetation and soil.

In this study, the cumulative anomaly method, Mann-Kendall test and sliding *t*-test were used to detect the abrupt climate change of the annual average temperature, precipitation and wind speed in the typical grassland, and the correct abrupt climate factors were obtained. The results show that although the Mann-Kendall test is simple to calculate, it is not suitable for detecting sequences with multiple mutation points. Therefore, this study uses three mutation test methods for cross-validation to improve the reliability of the test, so as to obtain the most accurate mutation year of climate elements. In addition, due to the vastness and complex topography of the study area, the 16 meteorological stations are not enough to cover the whole study. Therefore, it is necessary to use satellite meteorological data and numerical models to further analyze the spatial variation of climate change in typical steppe. This study only systematically analyzed the temporal and spatial distribution characteristics, abrupt phenomena and periodic rules of climate factors, and did not involve the influence factors that may cause climate change. So, the research focus of our team in the future should be the mechanism of climate change and the possible impact of climate change on vegetation ecology and land management.

6. Conclusions

In this study, the spatial and temporal evolution, abrupt changes and cyclical patterns of temperature, precipitation and maximum wind speed in the steppe area over the past 40 years were investigated based on observations of monthly temperature, precipitation and maximum wind speed at 16 meteorological stations on the typical grassland of Mongolian Plateau, using the linear trend method, cumulative anomaly method, Mann-Kendall test, sliding *t*-test, and Morlet wavelet analysis. The main results can be summarized as follows:

- (1) The spatial and temporal pattern evolution of temperature was studied. In the past 40 years, the annual average temperature of the typical grassland on the Mongolian Plateau showed a significant upward trend, with a climate tendency rate of $0.4\text{ }^{\circ}\text{C}/10\text{a}$ ($p < 0.001$), and the warming range gradually increased from northeast to southwest, with the most obvious warming in the southwest. The average temperature of the four seasons showed a warming trend, especially in spring and summer. The annual average temperature changed from low temperature to high temperature in 1992, and there was a significant 32-year cycle change.
- (2) The evolution characteristics of precipitation on different spatial and temporal scales were studied, and the annual precipitation showed a slightly decreasing trend with a climatic trend rate of $-2.39\text{ mm}/10\text{a}$. The precipitation change showed a decreasing trend at both ends, and precipitation increased in the middle region and the southern

part, while the precipitation decreased most obviously in the northern part. Among the seasonal variations, summer precipitation decreased the most. The annual precipitation changed from more to less in 1998, and there was a significant 29-year cycle change.

- (3) The temporal and spatial evolution characteristics of the maximum wind speed were clarified, and the annual average maximum wind speed showed a significant decreasing trend, with a climate trend rate of -0.33 m/s/10a ($p < 0.001$), and the maximum wind speed decreased most significantly in the south and northeast. In terms of seasonal variation, the average maximum wind speed decreased in all seasons, with the greatest decrease in spring. The annual average maximum wind speed changed from strong to weak around 1991, and there was a significant 28-year cycle change.
- (4) The decadal evolution of the typical steppe on the Mongolian Plateau was revealed. From the perspective of the whole study period, the typical steppe climate of the Mongolian Plateau is characterized by rising temperature, decreasing precipitation and decreasing maximum wind speed, which leads to the trend of warming and drying and weak weathering. In the past 40 years, the climate type showed a change process of “cold wet, strong wind–warm dry, weak wind”.

In conclusion, the research results firstly provide feasible and effective methods for the fine characterization of regional climate change. Secondly, they provide a reference for regional vegetation restoration and ecological security construction. Finally, they provide a scientific basis for the prediction of grazing capacity and the sustainable development of animal husbandry.

Author Contributions: Conceptualization, B.H.; methodology, S.Q. and C.S.; software, B.H. and C.S.; formal analysis, B.H.; resources, W.T. and L.N.; data curation, B.H.; writing—original draft preparation, B.H.; writing—review and editing, B.H., W.T., S.Q. and M.Y.; visualization, B.H.; supervision, W.T., S.Q. and T.K.; project administration, W.T., M.Y. and S.Q.; funding acquisition, W.T. All authors have read and agreed to the published version of the manuscript.

Funding: This research was funded by the National Nature Science Foundation of China (funder: Wulan Tuya, NO. 41861024 and funder: Mei Yong, NO. 41867070) and the Natural Nature Science Foundation of Inner Mongolia (funder: Si Qinchaoketu, NO. 2021BS04001).

Data Availability Statement: Not applicable.

Acknowledgments: The authors would like to thank the editors and anonymous reviewers for their valuable comments and suggestions which improved the quality of the manuscript.

Conflicts of Interest: The authors declare no conflict of interest.

References

1. Chen, S.; Yu, B.; Wu, R.; Chen, W.; Song, L. The dominant North Pacific atmospheric circulation patterns and their relations to Pacific SSTs: Historical simulations and future projections in the IPCC AR6 models. *Clim. Dyn.* **2020**, *56*, 701–725. [[CrossRef](#)]
2. Lynn, J.; Peeva, N. Communications in the IPCC's Sixth Assessment Report cycle. *Clim. Change* **2021**, *169*, 18. [[CrossRef](#)] [[PubMed](#)]
3. Ying, S. Impact of human activities on climate system: An interpretation of Chapter III of WGI report of IPCC AR6. *J. Atmos. Sci.* **2021**, *44*, 654–657. [[CrossRef](#)]
4. Huang, J.; Guan, X.; Ji, F. Enhanced cold-season warming in semi-arid regions. *Atmos. Chem. Phys.* **2012**, *12*, 5391–5398. [[CrossRef](#)]
5. Huang, J.; Ji, M.; Xie, Y.; Wang, S.; He, Y.; Ran, J. Global semi-arid climate change over last 60 years. *Clim. Dyn.* **2015**, *46*, 1131–1150. [[CrossRef](#)]
6. Huang, J.; Li, Y.; Fu, C.; Chen, F.; Fu, Q.; Dai, A.; Shinoda, M.; Ma, Z.; Guo, W.; Li, Z.; et al. Dryland climate change: Recent progress and challenges. *Rev. Geophys.* **2017**, *55*, 719–778. [[CrossRef](#)]
7. Liao, L.; Jiang, C.; He, B.; Liu, Q.; Zhu, F.; Cui, X. Response of vegetation coverage to climate change in Mongolian Plateau during recent 10 year. *Acta Ecol. Sin.* **2014**, *34*, 1295–1301. [[CrossRef](#)]
8. John, R.; Chen, J.; Ou-Yang, Z.-T.; Xiao, J.; Becker, R.; Samanta, A.; Ganguly, S.; Yuan, W.; Batkhisig, O. Vegetation response to extreme climate events on the Mongolian Plateau from 2000 to 2010. *Environ. Res. Lett.* **2013**, *8*, 035033. [[CrossRef](#)]
9. Liu, Z.; Wang, R.; Yao, Z. Air temperature and precipitation over the Mongolian Plateau and assessment of CMIP 5 climate models. *Resour. Sci.* **2016**, *38*, 956–969. [[CrossRef](#)]

10. Qin, F.-Y.; Jia, G.-S.; Yang, J.; Na, Y.-T.; Hou, M.-T.; Narenmandula. Spatiotemporal variability of precipitation during 1961–2014 across the Mongolian Plateau. *J. Mt. Sci.* **2018**, *15*, 992–1005. [[CrossRef](#)]
11. Hu, Q.; Pan, F.; Pan, X.; Zhang, D.; Li, Q.; Pan, Z.; Wei, Y. Spatial analysis of climate change in Inner Mongolia during 1961–2012, China. *Appl. Geogr.* **2015**, *60*, 254–260. [[CrossRef](#)]
12. Tong, S.; Zhang, J.; Bao, Y.; Wurina; Terigele; Weilisi; Lianxiao. Spatial and temporal variations of vegetation cover and the relationships with climate factors in Inner Mongolia based on GIMMS NDVI3g data. *J. Arid Land* **2017**, *9*, 394–407. [[CrossRef](#)]
13. Li, H.; Ma, L.; Liu, T. Change and relationship of temperature and precipitation in Inner Mongolia during 1951–2014. *J. Glaciol. Geocryol.* **2017**, *39*, 1098–1112. [[CrossRef](#)]
14. Davi, N.K.; Pederson, N.; Leland, C.; Nachin, B.; Suran, B.; Jacoby, G.C. Is eastern Mongolia drying? A long-term perspective of a multidecadal trend. *Water Resour. Res.* **2013**, *49*, 151–158. [[CrossRef](#)]
15. Nandintsetseg, B.; Greene, J.S.; Goulden, C.E. Trends in extreme daily precipitation and temperature near lake Hövsgöl, Mongolia. *Int. J. Climatol.* **2007**, *27*, 341–347. [[CrossRef](#)]
16. Sternberg, T.; Thomas, D.; Middleton, N. Drought dynamics on the Mongolian steppe, 1970–2006. *Int. J. Climatol.* **2011**, *31*, 1823–1830. [[CrossRef](#)]
17. Vandandorj, S.; Munkhjargal, E.; Boldgiv, B.; Gantsetseg, B. Changes in event number and duration of rain types over Mongolia from 1981 to 2014. *Environ. Earth Sci.* **2017**, *76*, 70. [[CrossRef](#)]
18. Angerer, J.; Han, G.; Fujisaki, I.; Havstad, K. Climate change and ecosystems of Asia with emphasis on Inner Mongolia and Mongolia. *Rangelands* **2008**, *30*, 46–51. [[CrossRef](#)]
19. Liu, S.; Wang, T. Climate change and local adaptation strategies in the middle Inner Mongolia, northern China. *Environ. Earth Sci.* **2011**, *66*, 1449–1458. [[CrossRef](#)]
20. Zhang, C.; Zhang, Y.; Li, J. Grassland Productivity Response to Climate Change in the Hulunbuir Steppes of China. *Sustainability* **2019**, *11*, 6760. [[CrossRef](#)]
21. Bao, G.; Liu, Y.; Liu, N.; Linderholm, H.W. Drought variability in eastern Mongolian Plateau and its linkages to the large-scale climate forcing. *Clim. Dyn.* **2014**, *44*, 717–733. [[CrossRef](#)]
22. Li, X.; Bai, M.; Yang, J.; Di, R.; Gao, Z. Risk zonation and evaluation of rainstorm and flood disasters in Inner Mongolia based on GIS. *J. Arid Land Resour. Environ.* **2012**, *26*, 71–77. [[CrossRef](#)]
23. Yulong, B.; Laiquan; Lina; Song, J.; Hujie; Yuhai, B.; Sachula. Analysis of Monitoring Method of Grassland Winter Drought Disaster Based on MOD10A1. *J. Catastrophol.* **2017**, *32*, 54–58. [[CrossRef](#)]
24. Liu, X.; Zhang, J.; Tong, Z.; Bao, Y.; Zhang, D. Grid-Based Multi-Attribute Risk Assessment of Snow Disasters in the Grasslands of Xilingol, Inner Mongolia. *Hum. Ecol. Risk Assess. Int. J.* **2011**, *17*, 712–731. [[CrossRef](#)]
25. Bao, C.; Yong, M.; Bi, L.; Gao, H.; Li, J.; Bao, Y.; Gomboludev, P. Impacts of Underlying Surface on the Dusty Weather in Central Inner Mongolian Steppe, China. *Earth Space Sci.* **2021**, *8*, e2021EA001672. [[CrossRef](#)]
26. Wang, H.; Li, Z.; Han, J. The spatial—Temporal change law of precipitation in Xilinguole steppe zone. *J. Arid Land Resour. Environ.* **2012**, *26*, 24–27. [[CrossRef](#)]
27. Qu, X.; Wu, H. Analysis of 53-year climate change characteristics of Hulun Buir city. *Res. Soil Water Conserv.* **2014**, *21*, 178–182. [[CrossRef](#)]
28. Qin, F.-Y. Study on the Response of the Temporal and Spatial Pattern of the Vegetation on the Mongolian Plateau to Climate Change. Ph.D. Thesis, Inner Mongolia University, Hohhot, China, 2019.
29. Dan, D. Climate Change on the Mongolian Plateau in the Past 35 years. Master’s Thesis, Inner Mongolia Normal University, Hohhot, China, 2014.
30. He, W.; Bu, R.; Xiong, Z.; Hu, Y. Characteristics of temperature and precipitation in Northeastern China from 1961 to 2005. *Acta Ecol. Sin.* **2013**, *33*, 519–531. [[CrossRef](#)]
31. Fu, C. The definition and detection of the abrupt climatic change. *Sci. Atmos. Sin.* **1992**, *16*, 482–493.
32. Wu, J.; Sheng, Z.; Du, J.; Zhang, Y.; Zhang, J. Spatiotemporal change patterns of temperature and precipitation in Northeast China from 1956 to 2017. *Res. Soil Water Conserv.* **2021**, *28*, 340–347. [[CrossRef](#)]
33. Kahya, E.; Kalaycı, S. Trend analysis of streamflow in Turkey. *J. Hydrol.* **2004**, *289*, 128–144. [[CrossRef](#)]
34. Zhang, Q.; Jiang, T.; Gemmer, M.; Becker, S. Precipitation, temperature and runoff analysis from 1950 to 2002 in the Yangtze basin, China. *Hydrol. Sci. J.* **2005**, *50*, 65–80. [[CrossRef](#)]
35. Miao, C.; Ni, J.; Borthwick, A.G. Recent changes of water discharge and sediment load in the Yellow River basin, China. *Prog. Phys. Geogr.* **2010**, *34*, 541–561. [[CrossRef](#)]
36. Zhang, J.; Wang, Y. Uncertainty analysis of rainfall-runoff relationship in Zhengzhou City. *Water Resour. Prot.* **2021**, *37*, 1–6. [[CrossRef](#)]
37. Kai, L.; Gege, N.; ZHANG, S. Study on the spatiotemporal evolution of temperature and precipitation in China from 1951 to 2018. *Adv. Earth Sci.* **2020**, *35*, 1113–1126. [[CrossRef](#)]
38. Xu, W.; Li, Q.; Jones, P.; Wang, X.L.; Trewin, B.; Yang, S.; Zhu, C.; Zhai, P.; Wang, J.; Vincent, L.; et al. A new integrated and homogenized global monthly land surface air temperature dataset for the period since 1900. *Clim. Dyn.* **2017**, *50*, 2513–2536. [[CrossRef](#)]
39. Zhang, Y. Analysis of Temporal-Spatial Variation Characteristics of Max Windspeed during 1976–2017 in Inner Mongolia. *Meteorol. J. Inn. Mong.* **2019**, *4*, 22–25. [[CrossRef](#)]

40. Ma, Z.; Yu, H.; Zhang, Q.; Cao, C. Characteristics and abrupt change of temperature and precipitation in inner Mongolia area over the period 1960–2016. *Res. Soil Water Conserv.* **2019**, *26*, 114–121. [[CrossRef](#)]
41. Li, X.; Han, G.; Guo, C. Impacts of climate change on dominant pasture growing season in central Inner Mongolia. *Acta Ecol. Sin.* **2013**, *33*, 4146–4155. [[CrossRef](#)]
42. Piao, J.; Chen, W.; Chen, S. Water vapour transport changes associated with the interdecadal decrease in the summer rainfall over Northeast Asia around the late-1990s. *Int. J. Climatol.* **2021**, *41*, E1469–E1482. [[CrossRef](#)]
43. Kang, X.; Cong-wen, Z.H.; Jin-hai, H. Impact of the Surface Air Temperature Warming around Lake Baikal on Trend of Summer Precipitation in North China in the Past 50 Years. *Plateau Meteorol.* **2011**, *30*, 309–317.
44. Zhu, Y.; Wang, H.; Zhou, W.; Ma, J. Recent changes in the summer precipitation pattern in East China and the background circulation. *Clim. Dyn.* **2010**, *36*, 1463–1473. [[CrossRef](#)]
45. Han, T.; Chen, H.; Wang, H. Recent changes in summer precipitation in Northeast China and the background circulation. *Int. J. Climatol.* **2015**, *35*, 4210–4219. [[CrossRef](#)]
46. Feng, K.; Ying, L.; Yi-fei, W.; Lili, L.; Lin, L.; Dong, L.; Yuan, X. Spatial and Temporal Variation Characteristics of Near-surface Gale Days in China from 1961 to 2016. *J. Anhui Agri. Sci.* **2017**, *45*, 188–196. [[CrossRef](#)]
47. Tong, S.; Liu, G.; Wu, N. Temporal spatial changes of temperature and precipitation in Xilingol League from 1961 to 2010. *Bull. Soil Water Conserv.* **2016**, *36*, 340–345. [[CrossRef](#)]
48. Liu, Y.; Zhuang, Q.; Chen, M.; Pan, Z.; Tchebakova, N.; Sokolov, A.; Kicklighter, D.; Melillo, J.; Sirin, A.; Zhou, G. Response of evapotranspiration and water availability to changing climate and land cover on the Mongolian Plateau during the 21st century. *Glob. Planet. Change* **2013**, *108*, 85–99. [[CrossRef](#)]
49. Miao, L.; Fraser, R.; Sun, Z.; Sneath, D.; He, B.; Cui, X. Climate impact on vegetation and animal husbandry on the Mongolian Plateau: A comparative analysis. *Nat. Hazards* **2016**, *80*, 727–739. [[CrossRef](#)]
50. Bailing, M.; Zhiyong, L.; Cunzhu, L.; Lixin, W.; Chengzhen, J.; Fuxiang, B.; Chao, J. Temporal and spatial heterogeneity of drought impact on vegetation growth on the Inner Mongolian Plateau. *Rangel. J.* **2018**, *40*, 113–128. [[CrossRef](#)]
51. Nanzad, L.; Zhang, J.; Tuvdendorj, B.; Yang, S.; Rinzin, S.; Prodhon, F.A.; Sharma, T.P.P. Assessment of Drought Impact on Net Primary Productivity in the Terrestrial Ecosystems of Mongolia from 2003 to 2018. *Remote Sens.* **2021**, *13*, 2522. [[CrossRef](#)]
52. Zhao, D.; Gao, X.; Wu, S.; Zheng, D. Trend of climate variation in China from 1960 to 2018 based on natural regionalization. *Adv. Earth Sci.* **2020**, *35*, 750–760. [[CrossRef](#)]